Molecular Biology of the Cell
Vol. 19, 807–821, March 2008

# A Lipid-mediated Quality Control Process in the Golgi Apparatus in Yeast

**Ludovic Pineau,* Laetitia Bonifait,† Jean-Marc Berjeaud,† Parissa Alimardani-Theuil,‡ Thierry Bergès,* and Thierry Ferreira***

*Université de Poitiers, Centre National de la Recherche Scientifique, Unité Mixte de Recherche 6161 "Transport des assimilats" and †Université de Poitiers, Centre National de la Recherche Scientifique, Unité Mixte de Recherche 6008 "Microbiologie fondamentale et appliquée," 86022 Poitiers Cedex, France

Submitted June 22, 2007; Revised November 6, 2007; Accepted December 10, 2007
Monitoring Editor: Sean Munro

**When heme biosynthesis is disrupted, the yeast *Saccharomyces cerevisiae* becomes unable to synthesize its major sterol, ergosterol, and desaturate fatty acids. We took advantage of this physiological peculiarity to evaluate the consequences of ergosterol and/or unsaturated fatty acid (UFA) depletions on the biogenesis of a model polytopic plasma membrane protein, the uracil permease Fur4p. We show that under UFA shortage, which results in low amounts of diunsaturated phospholipid species, and under ergosterol depletion, Fur4p is prematurely routed from the Golgi apparatus to the vacuolar lumen in a process that requires the ubiquitin ligase Rsp5p. Interestingly, this diversion is not correlated to Fur4p exclusion from detergent-resistant membranes. In an independent set of experiments, we show that Fur4p targeting to the plasma membrane depends on phosphatidylethanolamine amounts and more specifically on the propensity of this phospholipid to form a hexagonal phase. In light of recent literature, we propose a model in which ergosterol and diunsaturated phospholipid species maintain optimal membrane curvature for Fur4p to evade the Golgi quality control process and to be properly delivered to its normal destination.**

## INTRODUCTION

Because they are embedded in the membrane, polytopic plasma membrane proteins are highly sensitive to the composition of the lipid bilayer. Among cellular membranes, the plasma membrane displays a unique composition because, in addition to phospholipids, it contains two other classes of lipids to relatively high amounts, namely, sterols and sphingolipids (Hoekstra and van IJzendoorn, 2000). It has been proposed that this complex composition may result in lateral heterogeneity of the bilayer, a parameter that could influence the function and/or the biogenesis of membrane-anchored proteins. To give specificity to this broad concept, the existence of microdomains of specific composition has been suggested, among which "lipid rafts" have been the most popular (Jacobson *et al*., 2007). Lipid rafts are defined as sterol/sphingolipid enriched domains (Brown and London, 2000), and they display unique biophysical properties. They are thought to be formed by packing of the long saturated acyl chains of sphingolipids with cholesterol and to exist in a liquid-ordered (Lo) phase that can segregate from the bulk liquid-disordered (Ld) phase (for reviews, see Brown and London, 2000; London, 2005). This tight ordering of the saturated fatty acyl chains results in a relative resistance to detergent solubilization, hence their designation as detergent-resistant membrane fractions (DRMs).

In yeast, lipid rafts are proposed to assemble in the endoplasmic reticulum (ER) where they may serve as sorting platforms for several polytopic proteins destined for the cell surface (Bagnat *et al*., 2000). These include the plasma membrane ATPase Pma1p (Bagnat *et al*., 2000), the uracil permease Fur4p (Hearn *et al*., 2003), and three amino acid permeases: the general amino acid permease Gap1p (Lauwers and Andre, 2006), the tryptophane permease Tat2p (Umebayashi and Nakano, 2003), and the arginine permease Can1p (Malinska *et al*., 2003). Not surprisingly, affecting the composition of DRMs by depleting the cell of sterol and/or sphingolipids profoundly alters the biogenesis of raft-associated proteins (for review, see Helms and Zurzolo, 2004), albeit in different ways. The most common method to study the effects of raft disruption is to express the protein of interest in mutant strains altered in sphingolipid or ergosterol biosyntheses.

Interestingly, ergosterol depletion induces quite different behaviors depending on the protein studied. Indeed, when expressed in *erg6*Δ and *erg13*Δ cells, the tryptophan permease Tat2p is addressed to the endosomal pathway for vacuolar degradation, in a process that requires prior ubiquitylation by the Rsp5p–Bul1p complex. Under these conditions, Tat2p displays a loose association to DRMs (Umebayashi and Nakano, 2003). In contrast, the arginine permease Can1p is retained in the endoplasmic reticulum in an *erg24*Δ mutant and in unidentified intracellular compartments in an *erg6*Δ strain (Malinska *et al*., 2003), whereas Pma1p seems to be highly tolerant to ergosterol scarcity, because it is normally targeted to the plasma membrane in strains blocked at

This article was published online ahead of print in *MBC in Press* (http://www.molbiolcell.org/cgi/doi/10.1091/mbc.E07–06–0600) on December 19, 2007.

‡Present address: Université de Reims, Faculté des Sciences, "Laboratoire de microbiologie générale et moléculaire," Moulin de la Housse, BP 1039, 51687 Reims Cedex 2, France.

Address correspondence to: Thierry Ferreira (thierry.ferreira@univ-poitiers.fr).

Abbreviations used: ALA, δ-aminolevulinate; DRM, detergent-resistant membrane; UFA, unsaturated fatty acids.

**Table 1.** Yeast strains

| Strains | Characteristics | Source |
|---|---|---|
| *Y10000* | *MAT***a** *his3 leu2 met15 ura3* | Euroscarf |
| *hem1*Δ *a* | *MAT***a** *his3 leu2 trp1 ura3 hem1::LEU2* | Ferreira *et al.* (2004) |
| *hem1*Δ *α* | *MATα his3 leu2 trp1 ura3 hem1::LEU2* | Ferreira *et al.* (2004) |
| *hem1*Δ *end3*Δ | *MATα his3 leu2 ura3 hem1::LEU2 YNL084c::kanMX4* | This study, progeny of Y12992 (Euroscarf) x *hem1*Δ *a* |
| *hem1*Δ *rsp5-19$^{ts}$* | *MATα his3 leu2 ura3 lys2 trp1 hem1::LEU2 rsp5::HA-rsp5–19$^{ts}$* | This study, progeny of *rsp5-19$^{ts}$ MAT*α (Kaliszewski *et al*., 2006) x *hem1*Δ *a* |
| *hem1*Δ *sec7-1$^{ts}$* | *MATα ura3 lys2 trp1 sec7–1 hem1::LEU2* | This study, progeny of *sec7-1$^{ts}$ (Emr et al*., 1984) x *hem1*Δ *a* |
| *RY200T* | *MATα ura3-52 leu2-3, 112 his3-*Δ*200 trp1-D901 lys2-801 suc2-D9, GAL, psd1::TRP1 psd2::HIS3 dpl1:: KANR* | Robl *et al.* (2001) |

different levels of the ergosterol biosynthetic pathway (Gaigg *et al*., 2005).

A similar discrepancy between membrane proteins is observed under sphingolipid depletion induced in thermosensitive mutant *lcb1-100*. Lcb1p is required for serine palmitoyltransferase activity, essential for the first step in the synthesis of ceramide and sphingolipids (Buede *et al*., 1991). When expressed in *lcb1-100* cells, Pma1p loosens its association to DRMs and falls prey to a Golgi-based quality control mechanism to undergo vacuolar degradation (Bagnat *et al*., 2001). This may be due to the fact that Pma1p enters DRMs in an oligomeric form and that loss of sphingolipids in the *lcb1-100* strain compromises oligomer formation (Bagnat *et al*., 2001; Lee *et al*., 2002). Similarly, Can1p has been reported to be degraded in the vacuole in the *lcb1-100* mutant, whereas Fur4p only displays a delay in ER-to-plasma membrane targeting when expressed in this same mutant (Dupre and Haguenauer-Tsapis, 2003).

Recent work has also highlighted the role of fluid-phase components of the lipid bilayer, i.e., phospholipids, on the biogenesis of plasma membrane proteins. Indeed, Opekarova *et al*. (2005) reported that depleting the cells of phosphatidylethanolamine (PE) results in Can1p retention in the Golgi complex and of Pma1p in ER-derived structures. The authors suggested that the difference in Can1p and Pma1p behavior could be related to distinct immediate lipid surroundings of these two proteins, the so-called annular lipids (Lee, 2003).

Even if lipid raft formation in cells remains controversial (Munro, 2003; Valdez-Taubas and Pelham, 2003; London 2005; Jacobson *et al*., 2007), together, these studies clearly show that the biogenesis of integral proteins is intimately related to the composition and therefore the biophysical properties of membranes.

This is of particular significance given that cells often have to adjust their cellular lipid content in response to environmental changes. As an example, the yeast *Saccharomyces cerevisiae*, as a facultative anaerobe, can grow under low oxygen, provided that the medium is supplemented with ergosterol and an exogenous source of unsaturated fatty acids (UFAs). Indeed, several enzymes of the ergosterol pathway and Ole1p, the fatty acid desaturase, require heme as their prosthetic group, the synthesis of which is oxygen dependent (for review, see Daum *et al*., 1998). This implies significant readjustments of lipid homeostasis (Ferreira *et al*., 2004).

In the present study, we took advantage of this property to evaluate the relative consequences of ergosterol and/or UFA depletion on the biogenesis of a model polytopic plasma membrane protein, the uracil permease Fur4p.

## MATERIALS AND METHODS

### *Strains, Plasmids, and Culture Conditions*

The *S. cerevisiae* strains used in this study are listed in Table 1. Cells bearing the *hem1*Δ mutation were grown aerobically at 28°C in 1% *y*east extract (wt/vol), 1% *p*eptone (wt/vol), and 2% *raff*inose (wt/vol) (YPRaff) medium supplemented with 80 $\mu$g ml$^{-1}$ δ-aminolevulinate (ALA, aerobic-like conditions). Heme-induced lipid starved conditions (lipid depletion) were obtained by cultivating the cells in YPRaff medium without supplementation. Alternatively, YPRaff medium was supplemented with 80 $\mu$g ml$^{-1}$ ergosterol and/or 1% Tween 80 (vol/vol), used as the source of oleic acid. Where indicated, Tween 80 was replaced by myristoleic (C14:1), palmitoleic (C16:1), or oleic acid (C18:1) at a final concentration of 2 mM (Sigma, St. Louis, MO).

PE starvation conditions were obtained as described previously (Opekarova *et al*., 2002; Opekarova *et al*., 2005). RY200T cells were cultivated on YPRaff medium + ethanolamine 2 mM and transferred to 1% *y*east extract (wt/vol), 1% *p*eptone (wt/vol), and 4% *gal*actose (wt/vol) (YPGal) medium supplemented with ethanolamine, choline, or propanolamine at different concentrations for 16 h.

For Fur4p biogenesis studies, because the concentration of endogenous permease is too low to allow detection, and to specifically track the fate of newly synthesized permease under the different conditions, cells were transformed with the centromeric plasmid pFl38gF-green fluorescent protein (GFP), carrying a *FUR4* fusion gene, encoding Fur4p with a C-terminal GFP tag under the control of the inducible *GAL10* promoter (Marchal *et al*., 2002). Fur4p-GFP synthesis was induced by adding galactose to a final concentration of 4% (wt/vol).

For Pma1p immunolocalization studies, a hemagglutinin (HA)-tagged version of *PMA1* was placed under control of a heat-shock promoter in the integrative plasmid YIplac204 (*TRP*1; Yiplac204-2HSE$^{PT}$-HA-PMA1; Ferreira *et al*., 2002). As desired, expression of the tagged *PMA*1 gene was induced by incubation of the cells for 15 min at 39°C (Ferreira *et al*., 2002).

### *Lipid Analysis and Mass Spectrometry*

Lipid extracts were prepared from ≈2 × 10$^9$ (sterols), 2 × 10$^8$ (total fatty acids), or 10$^8$ (phospholipids) yeast cells, grown as indicated. Cells were harvested, washed with distilled water, suspended in 1 ml of cold water, and shock-frozen. They were broken by vigorous shaking with 500 $\mu$l of glass beads (diameter 0.3–0.4 mm; Sigma) by using a mini-beadbeater (Biospec Products, Bartlesville, OK) for 1 min at 5000 revolutions/min. Cellular lipids were extracted using chloroform:methanol (2:1, vol/vol) as described by Folch *et al*. (1957). The final organic phase was evaporated and lipids were dissolved either in 100 $\mu$l of hexane (sterols and total fatty acids) or 200 $\mu$l of chloroform:methanol:$H_2O$ (16:16:5, vol/vol/vol) (phospholipids).

Fatty acid methyl esters from total fatty acids were obtained as described by Ferreira *et al*. (2004). Briefly, lipids extracted from cells were submitted to a transesterification step, carried out by heating the samples at 50°C for 16 h in 2% (vol/vol) $H_2SO_4$ in dry methanol. The resulting fatty acid methyl esters were extracted with hexane and analyzed by gas chromatography by using a 25 m × 0.32 mm AT-1 capillary column (Alltech Associates, Deerfield, IL), with heptadecanoicmethyl ester as standard.

PE levels were determined exactly as described previously (Ferreira *et al*., 2004). After resolution on a precoated LK5 silica gel plate (Whatmann, Maidstone, United Kingdom) by using chloroform:ethanol:water:triethylamine (30:35:7:35, vol/vol/vol/vol) as the mobile phase, the various phospholipids species were visualized under UV by using a primuline solution. PE spots were scrapped from the plate before a transesterification step, as described above. PE amounts are expressed as nanomoles of fatty acids (FA) per 10$^9$ cells.

For specific sterol identification and quantification, total lipid extracts were subjected to saponification as reported previously (Ferreira *et al*., 2004). The

different sterol species were then separated by gas chromatography on the column described above, and identified by means of their retention times relative to cholesterol, used as a standard. The results are expressed as micrograms of sterol per $10^9$ cells.

For analyses by mass spectrometry (MS), total lipid extracts were reconstituted at a concentration of ~50 $\mu$g ml$^{-1}$ of phospholipids in chloroform: methanol:$H_2O$ (16:16:5, vol/vol/vol), with 1% (vol/vol) formic acid or diethylamine for analysis in the positive and negative ion modes, respectively. For routine single-stage MS, samples were analyzed with a triple quadrupole instrument model API 165 (PerkinElmerSciex Instruments, Boston, MA) equipped with an ion-spray source. Analysis of spectra was performed using the Biomultivew 1.2 software (PerkinElmerSciex Instruments), and raw identification of phospholipid species was done based on their expected $m/z$ by means of a homemade software program. The various species were unambiguously identified by tandem MS with a Deca XP Max equipped with an ion trap source (Thermo Electron, Waltham, MA) by precursor ion scan analysis, as described previously (Schneiter *et al*., 1999). Specifically, the molecular profile of phosphatidylcholine (PC) species was obtained by scanning for the positive ion precursors of $m/z$ 184, specific for choline phosphate. The molecular profile of inositol-containing lipids (i.e., phosphatidylinositol [PI] and inositol phosphoceramide [IPC]) was obtained by scanning for the negative ion precursors of $m/z$ 241, specific for the dehydration product of inositol phosphate (Schneiter *et al*., 1999).

### Isolation of Detergent-resistant Membranes

DRMs were isolated largely as described previously (Lauwers and Andre, 2006). Yeast cells ($10^8$) were lysed by vigorous shaking with 100 $\mu$l of glass beads (diameter 0.3–0.4 mm; Sigma) by using a mini-beadbeater (Biospec Products) for 1 min at 5000 revolutions/min in TNE buffer (50 mM Tris-HCl, pH 7.4, 150 mM NaCl, 5 mM EDTA, and 25 mM N-ethylmaleimide), supplemented with a cocktail of protease inhibitors (Sigma). The lysate (125 $\mu$l) was incubated with 1% Triton X-100 for 30 min on ice and adjusted to 40% iodixanol by adding 250 $\mu$l of OptiPrep (Axis-Shield, Oslo, Norway) before loading at the bottom of a two-step gradient (600 $\mu$l of 30% iodixanol in TXNE [50 mM Tris-HCl, pH 7.4, 150 mM NaCl, 5 mM EDTA, and 1% Triton X-100], 100 $\mu$l of TXNE). The gradient was centrifuged for 2 h at 200,000 $\times$ *g* in a TLA100-2 rotor (Beckman Coulter, Fullerton, CA). Six fractions of 175 $\mu$l were collected from the top of the gradient, and the proteins were precipitated by incubation with 10% trichloroacetic acid (TCA) for 30 min on ice. The precipitate was dissolved in a mix of 12.5 $\mu$l of 1 M Tris base and 12.5 $\mu$l of Laemmli buffer supplemented with 2% $\beta$-mercaptoethanol. Samples were heated at 37°C for 15 min, and then they were subjected to electrophoresis and analyzed by Western blot as described below. Signals were quantified using Scion Image (Scion, Frederick, MD).

### Invertase Secretion Assays

The invertase secretion assays were performed according to the method described by Munn *et al*. (1999). Yeast cells were grown as indicated to an $OD_{600}$ of 0.2–0.5 in selective medium containing 2% glucose. After washing, 10 $OD_{600}$ units of cells were induced for invertase expression by resuspension in selective medium containing 0.05% glucose and 2% sucrose. Cell samples were taken after 0, 15, 30, 45, and 60 min after transfer to low glucose medium. Invertase activity was determined as described by Munn *et al*. (1999), by using an enzyme reporter assay. Intracellular invertase activity was calculated by deducting extracellular activity, measured from unbroken cells, from total invertase, determined after prior permeabilization of the cells by freezing in liquid nitrogen in the presence of 10% Triton X-100.

### Total Protein Extracts and Immunoblotting

Total protein extracts were prepared as described by Volland *et al*. (1994). Logarithmic phase cells (0.5 OD) were suspended in 500 $\mu$l of water, broken by the addition of 50 $\mu$l 1.85 M NaOH; 3.5% (vol/vol) $\beta$-mercaptoethanol and proteins were precipitated by the addition of 50 $\mu$l of 50% (wt/vol) trichloroacetic acid. The resulting pellets were resuspended in 10 $\mu$l of 1 M Trizma base and 20 $\mu$l of Laemmli loading buffer, resolved on 10% polyacrylamide gels (SDS-polyacrylamide gel electrophoresis [PAGE]), and transferred to a nitrocellulose membrane for Western blot analysis. Fur4p-GFP was visualized by immunoblotting with an anti-GFP monoclonal antibody (Roche Diagnostics, Mannheim, Germany), diluted 1/1000, and enhanced chemiluminescence (ECL) detection. For quantification of Fur4p-GFP in the OptiPrep gradient fractions (see above), TCA-precipitated proteins were assayed in the same manner, but using an anti-GFP polyclonal antibody diluted 1/2000 before ECL detection; Pma1p was detected in these fractions by means of a polyclonal antibody (provided by Dr. C. W. Slayman, Yale University School of Medicine, New Haven, CT) diluted 1/2000.

### Fluorescence Microscopy

HA-tagged Pma1p was visualized by immunofluorescence essentially as described previously (Ferreira *et al*., 2002). The primary antibodies used were HA.11 monoclonal 16B12 from raw ascites fluid (BAbCO, Richmond, CA, University of California at Berkeley, CA), diluted 1:150; and Kar2p polyclonal antibody (provided by R. Schekman, University of California at Berkeley, CA), diluted 1:2500. Goat anti-rabbit fluorescein isothiocyanate (FITC) and goat anti-mouse Texas Red IgG (Jackson ImmunoResearch Laboratories, West Grove, PA) served as fluorescent secondary antibodies and were diluted 1:100.

For staining with *N*-[3-triethylammoniumpropyl]-4-[*p*-diethylaminophenylhexatrienyl] pyridinium dibromide (FM4-64), $10^7$ cells were incubated for 10 min at 4°C in 500 $\mu$l of a 10 $\mu$M FM4-64 solution in water. After washing to remove remaining soluble unbound stain, cells were incubated at 28°C for various times to visualize the plasma membrane, endosomes, and/or the vacuolar membrane.

Cells were observed on a Fluoview FV1000 confocal microscope (Olympus, Tokyo, Japan) by using dual-channel filters for simultaneous visualization of GFP signal (associated to the Fur4p–GFP fusion protein) and FM4-64, or FITC and Texas Red fluorescence. All images were taken with a 63$\times$ 1.4 numerical aperture Plan-Apochromat III DIC objective (Olympus). In time course experiments, or for direct comparison of GFP fluorescence after growth under different culture conditions, the exact same settings were used throughout the experiment to obtain a semiquantitative signal. Images were collected with FV10-ASW software (Olympus) and modified by contrast stretching, by using Adobe Photoshop 9.0 (Adobe Systems, San Jose, CA).

## RESULTS

### Under Sterol and UFA Depletion, Fur4p Falls Prey to a Golgi-based Quality Control Process

Under anaerobiosis, yeast cells are unable to synthesize UFAs, and their major sterol, ergosterol. Because anaerobiosis is difficult to achieve under standard laboratory conditions, we used a knockout mutant of ALA synthase (*hem1*Δ) as an experimental model (Verdiere *et al*., 1991). Such a strain can grow under standard oxygenated conditions, provided that the medium is supplemented with ALA (aerobic-like conditions). When transferred from aerobic-like conditions to unsupplemented YPD medium, *hem1*Δ cells display growth arrest as early as 5 h after the shift (Figure 1A; Ferreira *et al*., 2004). This arrest is related to dramatic changes in the cellular sterol and fatty acid patterns, compared with cells grown under aerobic-like conditions (Figure 1, B and C). As expected, ergosterol amounts decrease under these conditions (2-fold decrease compared with *hem1*Δ cells grown under aerobic-like conditions) and saturated fatty acids (myristic [C14:0], palmitic [C16:0] and stearic [C18:0] acids) accumulate at the expense of unsaturated forms (palmitoleic [C16:1] and oleic [C18:1] acids). This results in a drop of the fraction of UFA in cellular lipids (unsaturation ratio, Figure 1D) from 64.6 $\pm$ 1.7% to 47.7 $\pm$ 2.4%. After 7 h under the same conditions, these tendencies are amplified: ergosterol displays a fourfold decrease compared with aerobiosis and the unsaturation ratio falls down to 38.2 $\pm$ 1.6%. However, at this time point, *hem1*Δ cells can still be recuperated if ergosterol and oleic acid are added to the medium, which results in the restoration of a fatty acid unsaturation ratio and of ergosterol amounts similar to those observed for cells grown under aerobic-like conditions (see below). This shows that, among the various cellular consequences related to heme depletion, ergosterol and UFA starvation are the most detrimental for growth. For clarity in the text, *hem1*Δ cells grown in unsupplemented YPD medium will be referred to as "lipid-depleted."

We then evaluated the impact of heme-induced lipid depletion on the biogenesis of our model plasma membrane protein, the uracil permease Fur4p. To track the fate of newly synthesized Fur4p, we used a fully functional GFP-tagged version of the permease under the control of the inducible *GAL10* promoter (Marchal *et al*., 2002). *hem1*Δ cells were cultivated for 5 h (Figure 2A) or 7 h (Figure 2B) under aerobic-like conditions or under lipid depletion before galactose addition. After 5 h, fluorescence was detected at the plasma membrane as early as 60 min after supplementation of galactose to either growth conditions, and the overall

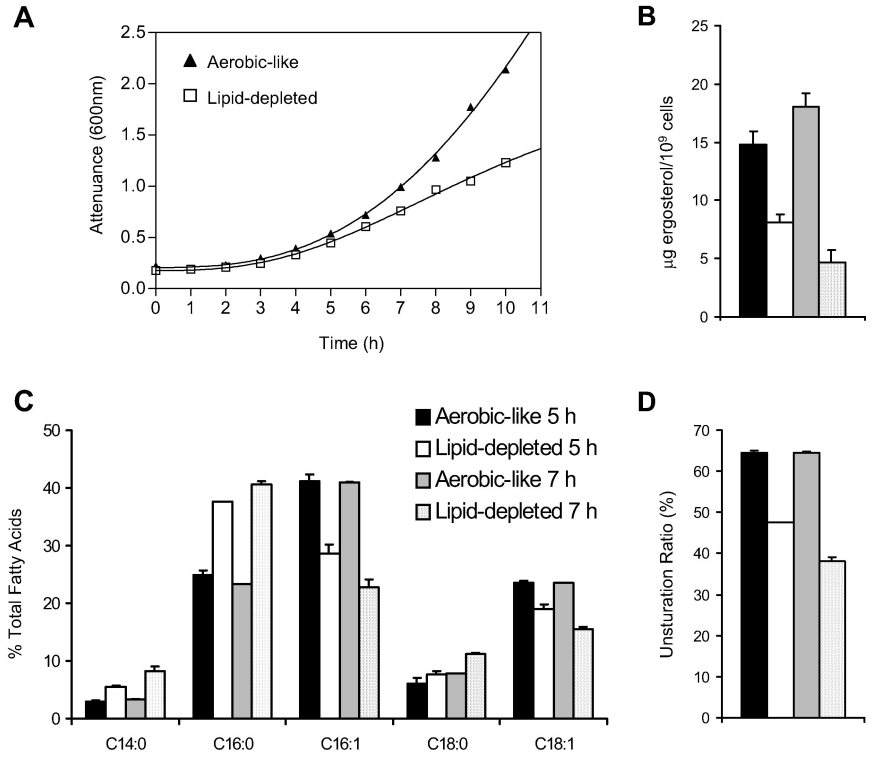


**Figure 1.** Consequences of heme depletion for cell growth, ergosterol, and fatty acid content. *hem1*Δ cells were grown to late exponential phase in YPD + ALA and shifted to fresh YPD medium (lipid-depleted) or YPD + ALA (aerobic-like). (A) Attenuance of the cultures was determined at the indicated time points after the shift. In parallel, the ergosterol (B) and fatty acid (C) content of the cells was determined 5 or 7 h after shift to fresh medium, as indicated and as described in *Materials and Methods*. Unsaturation ratio (D) corresponds to the percentage of UFA (C16:1 and C18:1). Values are means ± S. D. of at least three independent determinations.

fluorescence distribution was undistinguishable regardless of the lipid status of the cells throughout the entire experiment (Figure 2A). In contrast, when Fur4p-GFP synthesis was induced after 7 h of growth under lipid depletion, plasma membrane fluorescence could hardly be detected, even 120 min after galactose addition (Figure 2B), in contrast to aerobic-like conditions. In this case, fluorescence showed up as intracellular dot-like structures and as a diffuse disk that may correspond to the vacuolar lumen. These results indicate that a critical point is reached after 7 h under lipid-depleted conditions and that the lipid content of the cells is not compatible anymore with Fur4p-GFP delivery to and/or stability at the cell surface. Consistently, Fur4p-GFP amounts were also dramatically decreased under lipid de-

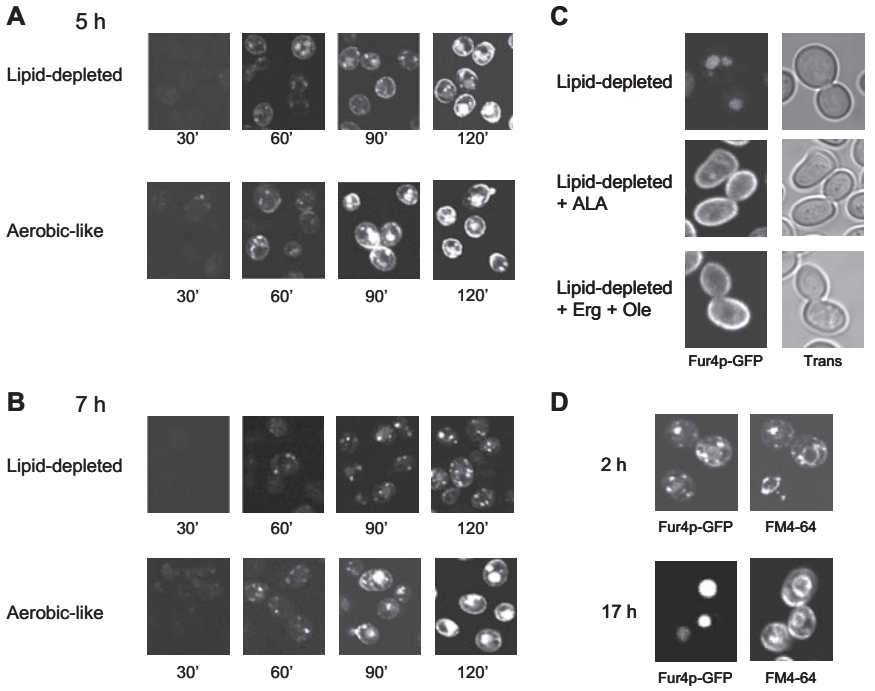


**Figure 2.** Impact of lipid depletion on Fur4p-GFP delivery to the cell surface. *hem1*Δ [pFl38gF-GFP] cells were grown to late exponential phase in YPRaff + ALA and shifted to fresh YPRaff (lipid-depleted) or YPRaff + ALA (aerobic-like). Fur4p-GFP synthesis was induced by adding galactose (4% final) to the medium after 5 h (A) or 7 h (B) after the shift. The GFP signal was visualized by confocal microscopy at the time indicated after galactose addition. (C) *hem1*Δ *end3*Δ [pFl38gF-GFP] cells were grown for 7 h under lipid-depleted conditions (YPRaff) before induction of Fur4p-GFP synthesis by galactose addition. After 3 h after Fur4p-GFP induction (i.e., after 10 h growth under lipid-depleted conditions), ALA (lipid-depleted + ALA), or ergosterol and Tween 80 (lipid-depleted + Erg + Ole) were added to the medium. GFP fluorescence was observed by confocal microscopy 24 h after shift to lipid-depleted conditions. The exact same settings were used throughout the experiment to obtain a semiquantitative signal. (D) *hem1*Δ [pFl38gF-GFP] cells grown for 7 h under lipid-depleted conditions as described in C. The GFP signal and FM4-64 cellular distribution were observed as described in *Materials and Methods* after 2 or 17 h after galactose addition. Trans, transmission.

pletion, as judged from Western blot quantification (Supplemental Figure S1). It should be noted that this situation was fully reversible, because adding ALA or ergosterol and oleic acid to the medium restored Fur4p targeting to the plasma membrane (Figure 2C).

To identify more precisely the compartments of Fur4p-GFP accumulation under lipid depletion, *hem1*Δ cells were incubated with the lipophilic styryl dye FM4-64 (Figure 2D), which specifically labels endocytic compartments and the vacuolar membrane (Vida and Emr, 1995). As shown in Figure 2D, 120 min after galactose addition (time 2 h), Fur4p-GFP and FM4-64 colocalized in dot-like structures corresponding to endosomes and, at the vacuole level, GFP signal was surrounded by the FM4-64 fluorescence that delineated the vacuolar membrane. Seventeen hours after induction of Fur4p-GFP synthesis under these conditions (i.e., 24 h after the shift to lipid-depleted conditions), the GFP signal was exclusively detected in the vacuolar lumen (Figure 2D, time 17 h). It was noticed that the lumenal signal was remarkably increased in *hem1*Δ *pep4*Δ cells (our unpublished data), which are defective in vacuolar protease activities (Woolford *et al*., 1986). Therefore, it seemed that under lipid depletion, Fur4p-GFP is delivered to the vacuolar lumen via the endosomal pathway for subsequent degradation.

We then questioned whether Fur4p-GFP could be sent to the vacuole after prior delivery to the plasma membrane and consecutive endocytosis. Endocytosis is a common mechanism for down-regulation of plasma membrane proteins (for review, see Dupre *et al*., 2004). To test this hypothesis, Fur4p-GFP was expressed in *end3*Δ cells, impaired in the internalization step of endocytosis (Benedetti *et al*., 1994). *hem1*Δ *end3*Δ were grown for 7 h under lipid-depleted conditions and Fur4p-GFP synthesis was induced by galactose addition (Figure 3A). As shown, no significant difference could be observed between *hem1*Δ *end3*Δ and *hem1*Δ cells grown under the same conditions (Figure 3A), i.e., no plasma membrane accumulation of the permease could be seen in the endocytosis defective mutant, whereas fluorescence was still detected in dot-like structures corresponding to endosomes and in the vacuolar lumen, as assessed by colocalization with FM4-64 (data not shown). This suggested that, under lipid depletion, newly synthesized permease is sent directly from an intracellular compartment to the vacuole for degradation, without prior cell surface delivery. This was confirmed by Western blot analysis of Fur4p-GFP amounts in *hem1*Δ and *hem1*Δ e*nd3*Δ cells grown under lipid-depleted conditions (Figure 3B). In the experiment depicted in this figure, *hem1*Δ and *hem1*Δ *end3*Δ cells were grown for 7 h in YPRaff medium before galactose addition. After 2 h under these conditions, cycloheximide was added to inhibit protein synthesis and Fur4p-GFP was detected by means of anti-GFP antibodies as a function of time. As shown, the permease was not protected from degradation in the endocytosis-deficient mutant, because Fur4p-GFP amounts rapidly decreased in both cell types.

It has been reported that newly synthesized permeases may be routed, entirely or in part, to the degradative vacuolar pathway without routing to the cell surface, depending on nutritional conditions. Fur4p itself is directly sorted from the Golgi apparatus to the endosomal system in response to uracil binding (Blondel *et al*., 2004). Accordingly, under lipid depletion, Fur4p was fully protected from degradation when blocked in the Golgi apparatus in a *hem1*Δ *sec7-1*$^{ts}$ double mutant at nonpermissive temperature (Figure 3B). This demonstrated that vacuolar degradation occurs after Fur4p exits from the Golgi apparatus, thereby ruling out ER-associated degradation.

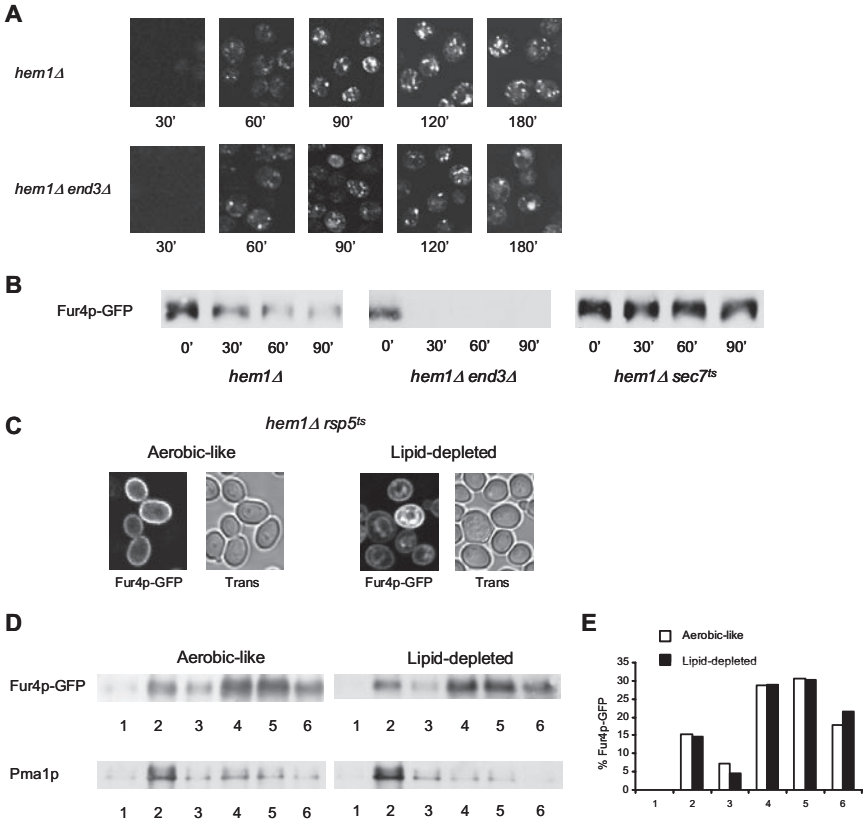


**Figure 3.** Characteristics of Fur4p-GFP trafficking under lipid depletion. (A) *hem1*Δ [pFl38gF-GFP] and *hem1*Δ *end3*Δ [pFl38gF-GFP] cells were cultivated exactly as in Figure 2B before visualization of GFP fluorescence. (B) *hem1*Δ [pFl38gF-GFP], *hem1*Δ *sec7*$^{ts}$ [pFl38gF-GFP], and *hem1 end3*Δ [pFl38gF-GFP] cells were grown for 7 h at 23°C under lipid depletion before transfer at 37°C and induction of Fur4p-GFP synthesis. After 2 h under these conditions, cycloheximide was added to the medium at a final concentration of 100 $\mu$g ml$^{-1}$ (t 0′). Total proteins were extracted from cells at the time indicated and the same amounts of protein were subjected to SDS-PAGE and Western blot analysis by using an anti-GFP antibody. (C) *hem1*Δ *rsp5*$^{ts}$ [pFl38gF-GFP] cells were grown in YPGal + ALA (aerobic-like) or YPGal (lipid-depleted) at 28°C for 24 h before visualization of GFP fluorescence by confocal microscopy. Trans, transmission. (D) *hem1*Δ *sec7*$^{ts}$ [pFl38gF-GFP] were grown under aerobic-like or lipid-depleted conditions for 7 h as indicated before induction of Fur4p-GFP synthesis. After 2 h after induction, cell lysates were subjected to Triton X-100 extraction and OptiPrep density gradient centrifugation. Six fractions were collected from the top of the gradient, TCA-precipitated, and analyzed by Western blot with anti-GFP and anti-Pma1p antibodies. (E) Fur4p-GFP signal in the fractions of the OptiPrep density gradient displayed in (D) has been quantified using the Scion Image software.

An early step for the delivery of vacuolar proteins to the lumen of this organelle occurs at the multivesicular body (MVB) level. MVB sorting begins at an endosomal compartment where a subset of proteins in the surrounding membrane is recognized and actively sorted into vesicles that bud into the lumen of the organelle (for review, see Katzmann *et al*., 2002). This process requires prior ubiquitylation by the ubiquitin ligase Rsp5p (Katzmann *et al*., 2004). In the case of uracil-induced diversion from the Golgi apparatus, ubiquitylation of Fur4p by the ubiquitin ligase Rsp5p also serves as a specific signal for its sorting to the luminal vesicles of the MVB (Blondel *et al*., 2004). As a consequence, Fur4p accumulates in the vacuolar membrane in the presence of uracil when expressed in an *rsp5*-deficient mutant (Blondel *et al*., 2004). Therefore, we investigated whether Rsp5p may play a similar role in Fur4p trafficking under lipid depletion. Fur4p-GFP was expressed in *hem1*Δ *rsp5-19$^{ts}$* cells incubated under aerobic-like conditions or in YPRaff medium at 28°C (Figure 3C). *rsp5-19$^{ts}$* displays a point mutation resulting in a single amino acid change in the ww3 domain of Rsp5p (Kaliszewski *et al*., 2006), a domain essential for MVB sorting of some vacuole lumenal proteins (Morvan *et al*., 2004). This allele confers significant growth delay to the cells at 28°C and complete growth arrest at 37°C (Kaliszewski *et al*., 2006). Under aerobic-like conditions, Fur4p-GFP was only detected at the periphery of the cells (Figure 3C). This is due to the fact that Rsp5p ubiquitylation of Fur4p is a prerequisite for its removal from the plasma membrane by endocytosis (Hein *et al*., 1995). As expected, the permease could be detected in the vacuolar membrane under lipid depletion, showing that, as observed for uracil-induced endosomal targeting of the permease (Blondel *et al*., 2004), Rsp5p is required for Fur4p to enter the intraluminal vesicles of the MVB. Interestingly, under these conditions, Fur4p-GFP was also detected at the plasma membrane level (Figure 3C). Thus, the two fates of Fur4p sorting under lipid limitation, i.e., the cell surface-targeting defect and the delivery to the vacuolar lumen, are simultaneously affected in the *rsp5*-defective mutant. Whether the observed plasma membrane targeting results from rerouting of Fur4p-GFP to the "normal" secretory pathway or to an alternative endosomal route (Gabriely *et al*., 2007), such as already postulated for Tat2p (Umebayashi and Nakano, 2003), will require further investigation.

It has previously been proposed that affecting raft integrity can induce plasma membrane proteins to undergo a Golgi-based quality control process (Bagnat *et al*., 2001; Wang and Chang, 2002; Umebayashi and Nakano, 2003). A well-documented example is the tryptophane permease Tat2p that is diverted from the Golgi apparatus to the endosomal system under conditions of ergosterol depletion, i.e., when expressed in a mutant deleted for the *ERG6* gene encoding the Delta(24)-sterol C-methyltransferase (Umebayashi and Nakano, 2003). In the case of Tat2p, targeting to the endosomal pathway in *erg6*Δ cells was related to a loose association of the permease with DRMs (Umebayashi and Nakano, 2003). Detergent insolubility of Fur4p was therefore examined under aerobic-like and lipid-depleted conditions by treatment with Triton X-100 followed by a flotation analysis on an OptiPrep gradient (Figure 3D). It has to be noted that the experiment displayed in this figure was performed on *sec7$^{ts}$* cells (see above) grown at a nonpermissive temperature, i.e., under conditions where Fur4p-GFP is stopped at the branch line between the endosomal and the plasma membrane pathways. In these cells, Fur4p is protected from degradation under lipid depletion (Figure 3B), due to its retention in the Golgi complex. Surprisingly, the patterns of Fur4p-GFP on the OptiPrep gradient were identical under both conditions (Figure 3, D and E): at the cell/detergent ratio used in this experiment ($\sim 10^9$ cell ml$^{-1}$ incubated with 1% Triton X-100), Fur4p-GFP was detected to significant levels in fractions 2 and 3 that correspond to DRM associated forms (15 and 7% of total Fur4p-GFP signal, respectively; Figure 3E), but also in fractions 4, 5, and 6, corresponding to solubilized material. Similarly, the plasma membrane proton ATPase Pma1p, which is a well-established DRM-associated protein (Bagnat *et al*., 2000, 2001), displayed similar behavior under both aerobic-like and lipid-depleted conditions, but it was almost exclusively detected in fraction 2, in contrast to Fur4p. The observed ambivalent distribution of Fur4p suggests that the permease association to DRMs is not as tight as that of Pma1p. However, our results clearly show that Fur4p association to DRMs is not affected under lipid depletion, and that a weaker association to DRMs can therefore not account for Fur4p sorting to the endosomal system, in contrast to what has been proposed for Tat2p.

### *Fur4p Failure to Reach the Plasma Membrane under Lipid Depletion Is Not Due to a General Block of the Secretory Pathway*

To assess whether heme-induced lipid depletion could result in a global defect of the secretory pathway, the secretion of invertase was measured under the same conditions. Internal and external invertase activities were determined using enzyme latency assays, as described previously (Munn *et al*., 1999). As a control, invertase secretion was also measured in cells grown under conditions of normal Fur4p delivery to the plasma membrane, i.e., under aerobic-like conditions (Figure 4A). As shown in Figure 4A, lipid depletion did not significantly alter the kinetics of invertase secretion because no intracellular accumulation could be detected. In contrast, the same experiments were performed in a *sec14* thermosensitive mutant, defective in Golgi export of secreted proteins at nonpermissive temperature (Henneberry *et al*., 2001). Such a mutant was unable to secrete invertase into the periplasm, but rather accumulated intracellular invertase at 37°C (Figure 4A).

We also evaluated whether lipid depletion could impair the trafficking of integral plasma membrane proteins in general, by monitoring the biogenesis of the proton ATPase Pma1p under these conditions (Figure 4B). For this purpose, a HA-tagged version of Pma1p under control of a heat-shock promoter was used (DeWitt *et al*., 1998; Ferreira *et al*., 2002), that allows its synthesis by transient shifting at elevated temperature. The newly synthesized protein can be tracked by immunofluorescence using an anti-HA antibody (DeWitt *et al*., 1998; Ferreira *et al*., 2002). In the experiment displayed in Figure 4B, cells grown for 7 h under aerobiosis-like and lipid-depleted conditions were shifted to 39°C for 15 min and Pma1p-HA was visualized after 1 h after the shift. Interestingly, Pma1p-HA could be detected at the cell periphery under both conditions, showing that, in contrast to Fur4p, ergosterol and UFA limitations do not abolish Pma1p delivery to the plasma membrane. These results were to a certain extent expected, because Pma1p plasma membrane delivery and stability at this level seem to be directly coupled to its association to DRMs (Bagnat *et al*., 2001; Pizzirusso and Chang, 2004; Gaigg *et al*., 2005, 2006) and DRM association of Pma1p was not impaired under lipid depletion (Figure 3D).

Therefore, Fur4p-GFP diversion from the Golgi apparatus to the endosomal pathway under heme-induced lipid limitation is not due to a blockage of the secretory pathway nor

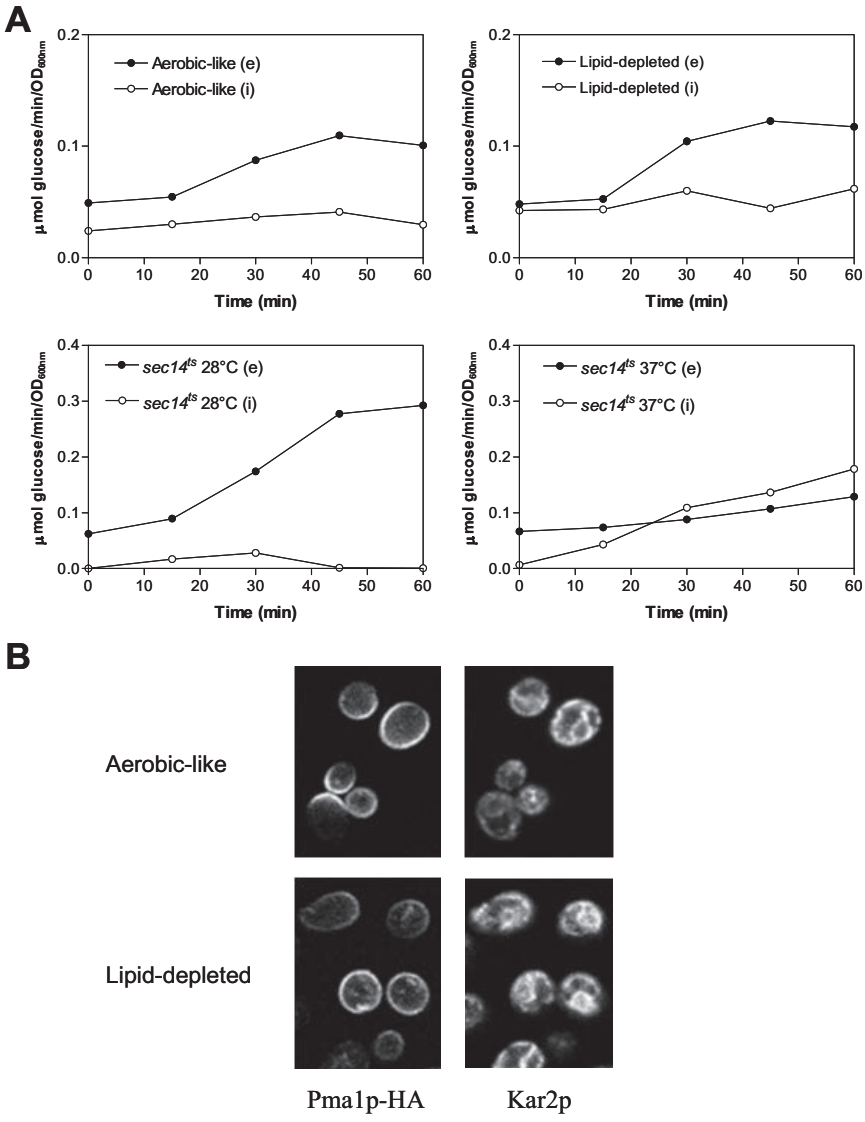


**Figure 4.** Consequences of lipid depletion on invertase secretion and Pma1p plasma membrane targeting. (A) *hem1*Δ cells (top) were grown as described in the legend of Figure 1 for 7 h in YPD +ALA (aerobic-like) or YPD (lipid-depleted) before invertase induction. *sec14*$^{ts}$ cells (bottom) were grown to exponential phase at 28°C and invertase was induced by glucose limitation in cells maintained under permissive conditions (28°C) or transferred to nonpermissive temperature (37°C). Samples were removed at the time points indicated and the activity of internal and secreted invertase was determined as described in *Materials and Methods*. Closed symbols, extracellular invertase activities (e); open symbols, intracellular invertase activities (i). (B) *hem1*Δ [Yiplac204–2HSE$^{pr}$-HA-PMA1] cells were grown under aerobic-like or lipid-depleted conditions for 7 h before incubation for 15 min at 39°C for induction of Pma1p-HA synthesis. Sixty minutes after the heat shock, the cells were fixed and processed for immunofluorescence with antibodies to HA (left). Anti-Kar2p antibodies were used as nonspecific markers to visualize the cells in the microscope field (right).

to a nonspecific effect on the biogenesis of plasma membrane proteins.

### *Individual Sterol and UFA Depletions Result in Direct Targeting of Fur4p to the Endosomal Pathway*

In a next step, we questioned the individual contributions of ergosterol and UFA shortage on Fur4p recognition by the Golgi quality control process. To answer this question, Fur4p-GFP trafficking was analyzed under conditions of heme-induced ergosterol or UFA starvation, by selectively adding oleate to the medium, as the source of UFA (ergosterol depletion; Figure 5A, + Ole), or ergosterol (UFA depletion; Figure 5A, + Erg). As a control, heme-depleted cells were also incubated with both lipid molecules (Figure 5A, + Erg + Ole). As expected, adding both ergosterol and UFAs to the medium allowed targeting of Fur4p-GFP to the cell surface (Figure 5A, bottom, time 180 min). Surprisingly, individual depletion of ergosterol or UFAs both prevented Fur4p delivery to the plasma membrane (Figure 5A). Instead, the fluorescence was mainly detected in the vacuolar lumen, as determined via colocalization with FM4-64 (Figure 5B). As in the case of dual depletion, plasma membrane accumulation was not observed in *hem1*Δ *end3*Δ when UFA or ergosterol were omitted (Figure 5C), and the permease was detected in the vacuolar membrane in *hem1*Δ *rsp5-19*$^{ts}$ at nonpermissive temperature in both cases (Figure 5D). Altogether, these experiments show that individual depletion of ergosterol or UFA results in Fur4p channeling to the Golgi-based quality control process.

### *UFA Depletion Induces the Accumulation of Short Saturated Fatty Acyl Chains in Phospholipids*

Given the similar consequences of ergosterol and UFA shortage on Fur4p-GFP trafficking, it was important to evaluate the precise impact of these depletions on the overall lipid composition of the cells. In a first step, the ergosterol cellular content was analyzed under the different conditions (Figure 6A). As expected, when heme synthesis was inhibited, the absence of an exogenous source of sterol resulted in ergosterol scarcity (Figure 6A, lipid-depleted and + Ole), whereas cellular ergosterol pools were fully replenished when this molecule was added to the medium, regardless of the presence or the absence of exogenously supplied UFA (Figure 6A, compare + Erg and + Erg + Ole).

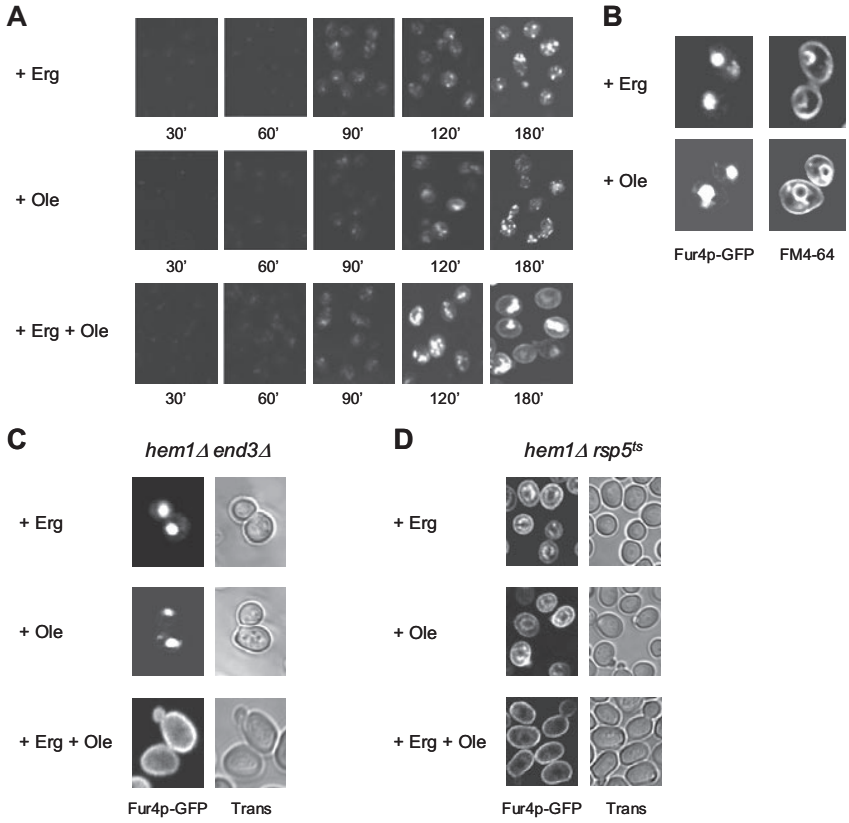


**Figure 5.** Relative impacts of ergosterol and UFA shortage on Fur4p-GFP biogenesis. (A) *hem1*Δ [pFl38gF-GFP] cells were cultivated to late exponential phase in YPRaff + ALA before shift to fresh YPRaff + ergosterol (+ Erg), YPRaff + Tween 80 (+ Ole), or YPRaff + ergosterol + Tween 80 (+ Erg + Ole). After 7 h under these conditions, Fur4p-GFP synthesis was induced and cellular GFP distribution was observed at the time indicated after induction. (B) After growth as described in A and 180 min after Fur4p-GFP induction, cells were incubated with FM4-64 before visualization by confocal microscopy. *hem1*Δ *end3*Δ [pFl38gF-GFP] (C) and *hem1*Δ *rsp5*$^{ts}$ [pFl38gF-GFP] (D) cells were grown as described in Figure 3C. + Erg, YPGal + ergosterol; + Ole, YPGal + Tween 80; and + Erg + Ole, YPGal + ergosterol + Tween 80. Trans, transmission.

Subsequently, phospholipid species were analyzed by mass spectrometry as described in *Materials and Methods*. A comparison of positive ion mode spectra is displayed in Figure 6B. For peak assignment, ions were subjected to ion scan analyses as described previously (Schneiter *et al*., 1999). In this figure, the main peaks corresponding to molecular species of PC are indicated. As shown, cells grown under UFA depletion (lipid-depleted and + Erg) displayed very similar patterns, with the accumulation of low $m/z$ PC molecular species, corresponding to PC molecules bearing short saturated acyl chains (PC 24:0, 26:0, 28:0, and 30:0). Interestingly, these species were hardly detectable under aerobic-like conditions or when oleate was added to the medium (+ Ole and + Erg +Ole, Figure 6), showing a direct correlation between the accumulation of short fatty acyl chains and UFA scarcity. Such an accumulation of short chains was also observed for other phospholipid species, i.e., PE, phosphatidylserine (PS) and PI under UFA depletion (unpublished data).

Detailed analysis of PC species under the different conditions is displayed in Figure 7A. As shown, significant differences can be observed in PC composition between the treatments. Overall, these rearrangements of PC species can be visualized by the monitoring of three parameters, namely the unsaturation ratio (Figure 7B), the average number of carbons in the acyl chains (average chain length; Figure 7C) and the relative quantities of saturated, monounsaturated and diunsaturated species (Figure 7D).

As shown in these figures, UFA depletion (lipid-depleted and + Erg) modified all three parameters compared with cells grown under aerobic-like conditions, with a decrease in the average length of fatty acyl chains (Figure 7C) and a reduction of the unsaturation ratio (Figure 7B) related to an increase in saturated species at the expense of diunsaturated forms (Figure 7D). These modifications are the consequence of the accumulation of PC species bearing short saturated chains (PC 24:0, 26:0, 28:0, and 30:0) at the expense of diunsaturated species (PC 32:2 and 34:2), that are predominant in cells grown under aerobic-like conditions (Figure 7A).

Interestingly, oleate supplementation (+ Ole and Erg + Ole) not only restored the unsaturation ratio, but all three parameters, albeit PC species in cells grown under these conditions tended to display longer fatty acyl chains than PC species extracted from aerobically grown cells (Figure 7C). This ought to be related to the accumulation of PC 34:1 and PC 36:1 species at the expense of PC 32:2 under these conditions, due to increased incorporation of oleate (C18:1) in phospholipids (Figure 7A). However, because all three parameters are nearly identical in UFA competent cells, whatever the origin of the UFA source (i.e., endogenous or exogenous), one may assume that the biophysical properties of the phospholipid bilayer might be very similar, at least in terms of width and relative fluidity. This may explain why normal growth and plasma membrane delivery of Fur4p were observed under haem depletion when oleate and ergosterol were added to the medium (Figure 5A, + Erg + Ole).

It was shown recently that the synthesis of sphingolipids up to IPC was essential for Pma1p association to DRMs and its subsequent delivery and/or stability at the plasma membrane level (Gaigg *et al*., 2005). The core of sphingolipids are ceramides that are constituted in yeast by a long chain base (mainly phytosphingosine), condensed with a C26 very long chain fatty acid (for recent review, see Dickson *et al*., 2006). More specifically, Gaigg *et al*. (2006) have demonstrated that the fatty acyl chain length of IPC was crucial for Pma1p biogenesis, rather than the polar head groups of the sphingolipid molecule.

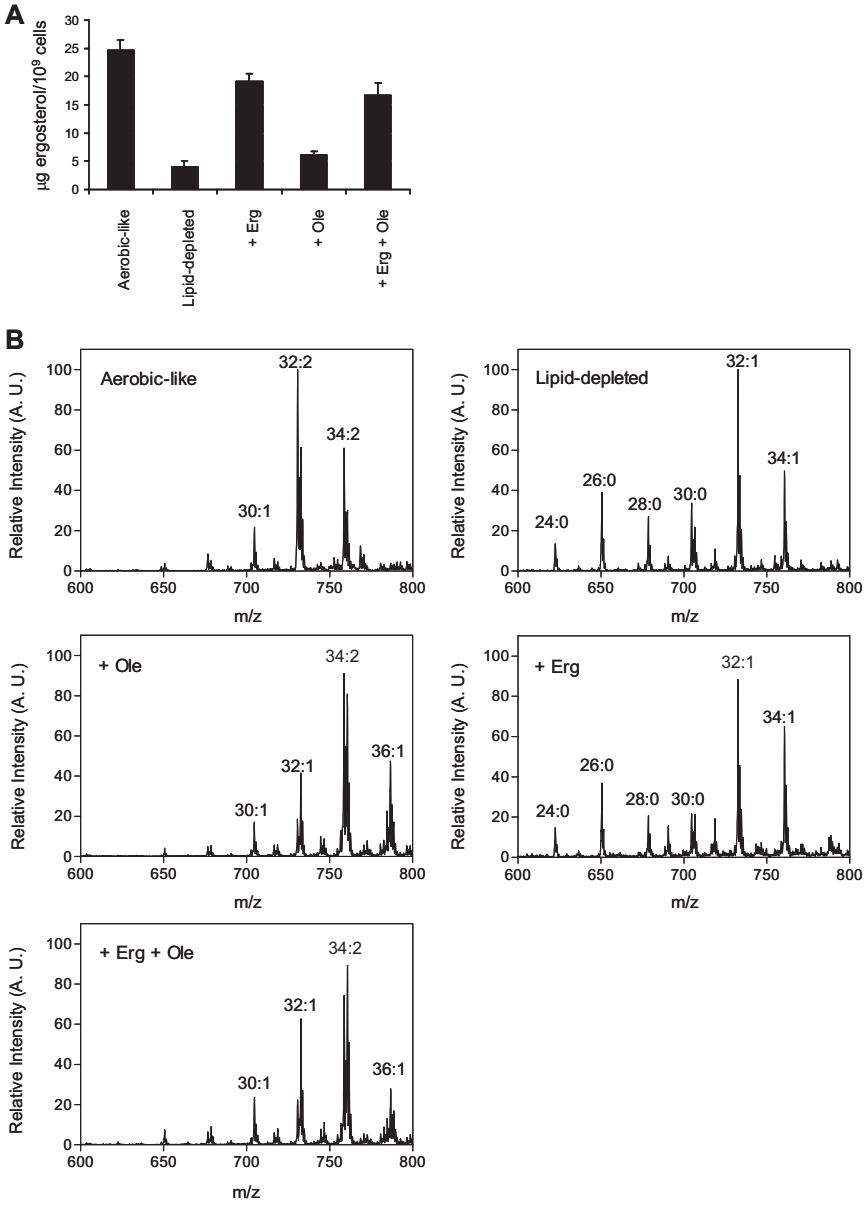


**Figure 6.** Lipid composition of *hem1*Δ cells under the different conditions. *hem1*Δ cells were grown in YPD (lipid-depleted), YPD + ALA (aerobic-like), YPD + ergosterol (+ Erg), YPD + Tween 80 (+ Ole) or YPD + ergosterol + Tween 80 (+ Erg + Ole). After 7 h under these conditions, lipids were extracted from the cells for analysis. (A) Ergosterol amounts were quantified as described in *Materials and Methods* and are expressed as $\mu$g ergosterol/$10^9$ cells. Values are means ± S. D. of at least three independent measurements. (B) Positive ion mass spectra of the $m/z$ range 600–800. The total carbon chain length (x) and number of carbon–carbon double bonds (y) of PC molecular species is indicated (x:y). A.U., arbitrary units.

Although unlikely, because Pma1p was effectively targeted to the plasma membrane and Fur4p and Pma1p were normally associated to DRMs, we wondered whether short fatty acyl chain accumulation could occur in sphingolipids as in phospholipids, and whether it may have accounted, at least in part, for Fur4p mislocalization. To address this question, lipids extracted from cells cultured under the different conditions were analyzed by mass spectrometry in the negative ion mode. The obtained spectra are displayed in Figure 8. Under these conditions, PI species could be visualized as well as the mature sphingolipid forms IPC-C and IPC-B/B′ that differ from each other by one hydroxyl group. PI and IPC species were unambiguously identified by negative precursor scans for $m/z$ 241, specific for the dehydration product of inositol phosphate (Schneiter *et al.*, 1999). Interestingly, whatever the condition tested, the main IPC-B/B′ and IPC-C species detected displayed the same $m/z$, i.e., 936 and 952 Da respectively, which correspond to C26 fatty acid containing species. Moreover, the intensities of the corresponding peaks were significantly higher, relative to the ones of PI species, for cells cultivated under UFA depletion (Figure 8, lipid-depleted and + Erg). Because PI amounts were similar for cells grown under haem deficiency, whatever the supplement added to the medium (lipid-depleted, + Erg, + Ole, +Erg + Ole; data not shown), these results showed that UFA starvation did not result in decreased IPC amounts. Therefore, we conclude that Fur4p mistargeting to the endosomal system under UFA depletion (Figure 5, lipid-depleted, + Erg) cannot be due to low IPC amounts nor to a shortening of the fatty acyl component of sphingolipids.

### *The Unsaturation Ratio of Fatty Acyl Chains of Phospholipids, but Not Their Length, Is Crucial for Fur4p to Evade the Golgi Quality Control Process*

UFA depletion induces both a shortening of fatty acyl chains in phospholipids and a decrease in their unsaturation level (Figure 7). To evaluate the respective consequences of these

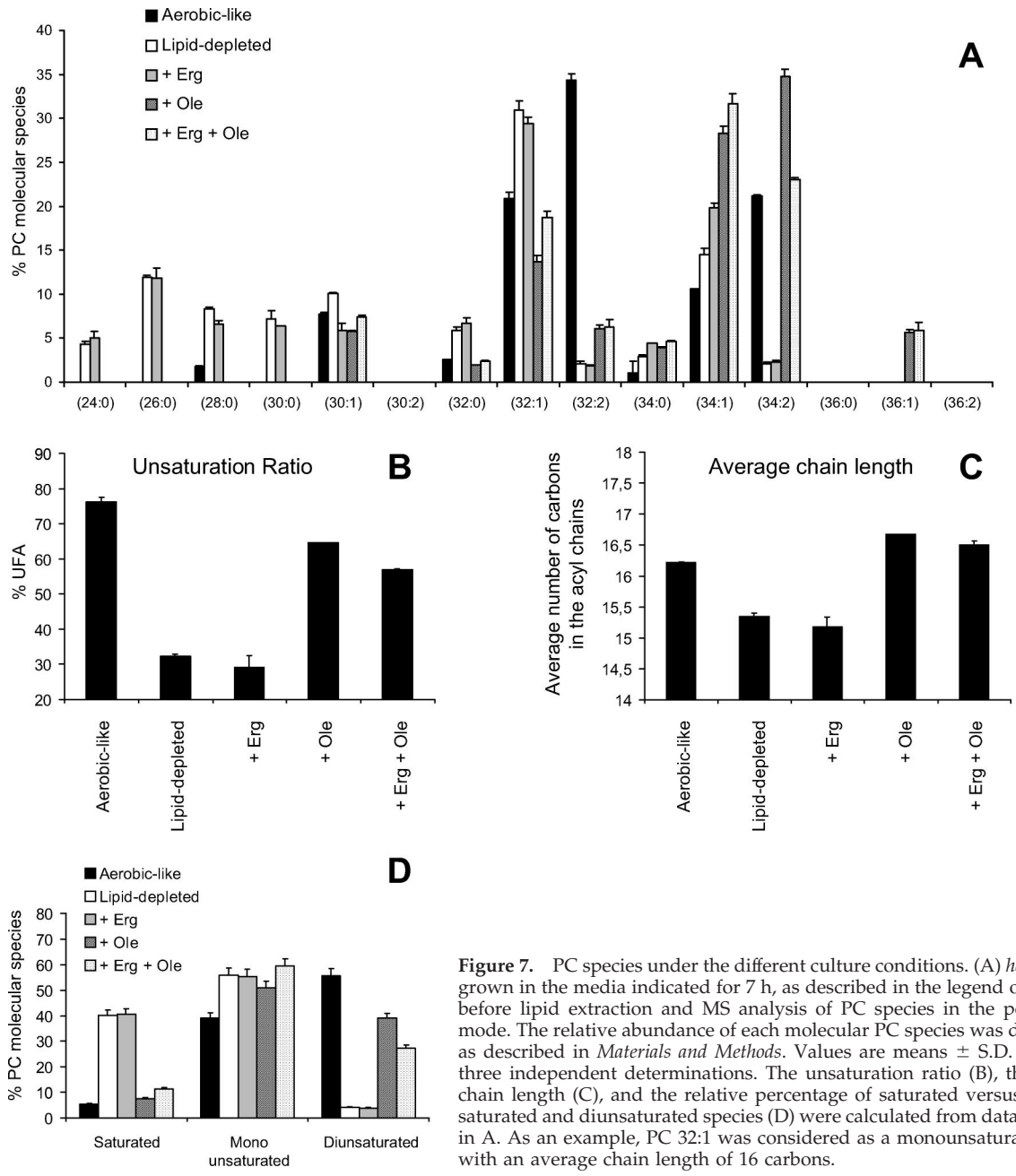


**Figure 7.** PC species under the different culture conditions. (A) *hem1*Δ were grown in the media indicated for 7 h, as described in the legend of Figure 6, before lipid extraction and MS analysis of PC species in the positive ion mode. The relative abundance of each molecular PC species was determined as described in *Materials and Methods*. Values are means ± S.D. of at least three independent determinations. The unsaturation ratio (B), the average chain length (C), and the relative percentage of saturated versus monounsaturated and diunsaturated species (D) were calculated from data displayed in A. As an example, PC 32:1 was considered as a monounsaturated specie with an average chain length of 16 carbons.

parameters for Fur4p-GFP trafficking, *hem1*Δ cells were grown in media supplemented with fatty acids of increasing chain length, namely, myristoleic (C14:1), palmitoleic (C16:1), and oleic acid (C18:1). As shown in Figure 9A, Fur4p-GFP could be detected at the plasma membrane level regardless of the length of the exogenously supplied UFAs. The Fur4p-GFP signal at the plasma membrane in the presence of C14:1 was even more visible when permease molecules that escaped the Golgi quality control process were stabilized at the cell periphery in the endocytosis-defective *hem1*Δ *end3*Δ strain (Figure 9B). This suggested that fatty acyl chain length was not a determinant parameter of the lipid-mediated Golgi quality control process. To rule out the possibility that exogenous fatty acids could have been further elongated by cellular elongases before their incorporation in phospholipids, phospholipids extracted from cells grown on ergosterol and C14:1 (+ Erg + 14:1) were analyzed by electrospray ionization-mass spectrometry (ESI-MS). The results obtained for PC under these conditions and under UFA depletion (+ Erg) are displayed in Figure 10A. As shown, growth on C14:1 induced the accumulation of short diunsaturated species, such as C28:2 and C30:2. As a result, the unsaturation ratio was restored to normal by the addition of C14:1 compared with cells grown under UFA depletion, because an identical value was obtained with aerobically grown cells (Figure 10B), whereas the average chain length was maintained at 15.5 carbon atoms (Figure 10C). Because unsaturated phospholipids generate bilayers of smaller width than saturated phospholipids, due to loose packing of unsaturated fatty acyl chains, we conclude that growth on C14:1 does not compensate for the global shortening of fatty acyl chain length induced by UFA depletion. Rather, C14:1 likely

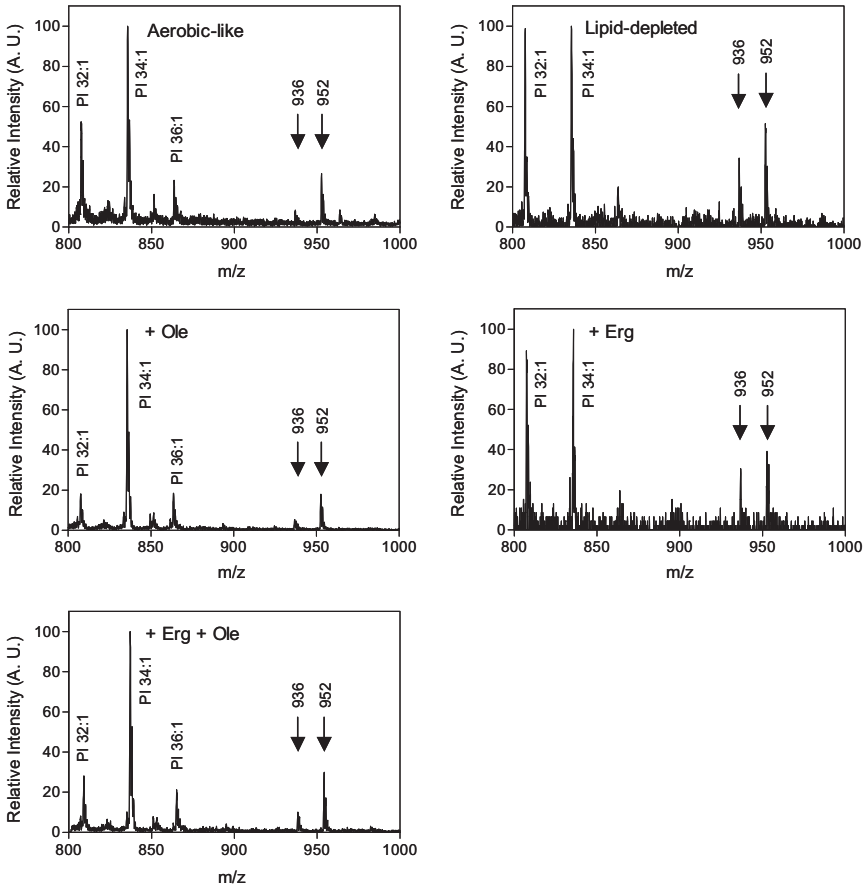


**Figure 8.** Inositol phosphoceramide species under the various culture conditions. *hem1*Δ cells were grown in the media indicated for 7 h before lipid extraction, and MS analysis in the negative ion mode. The main PI, IPC-B/B′ ($m/z$ = 936 Da), and IPC-C ($m/z$ = 952 Da) species are indicated. A.U., arbitrary units.

corrects Fur4p targeting to the plasma membrane by restoring a high unsaturation level of fatty acids in phospholipids, and more specifically by restoring elevated levels of diunsaturated species (Figure 10D), equivalent to that observed under aerobic-like conditions.

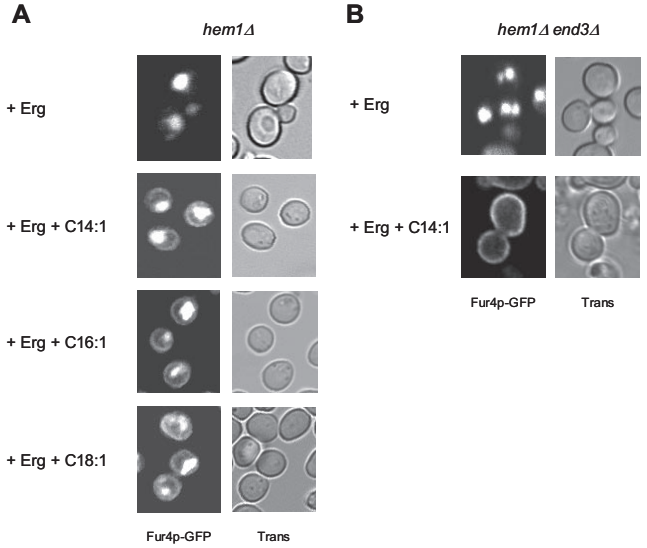


**Figure 9.** Impact of fatty acid chain length of Fur4p-GFP plasma membrane delivery. *hem1*Δ [pFl38gF-GFP] (A) or *hem1*Δ *end3*Δ [pFl38gF-GFP] (B) cells were grown for 24 h in YPGal medium + ergosterol eventually supplemented with myristoleic acid (C14:1), palmitoleic acid (C16:1), or oleic acid (C18:1) as indicated, before visualization of GFP fluorescence. Trans, transmission.

### *Hexagonal Phase Propensity of Phosphatidylethanolamine Is Required for Fur4p Delivery to the Plasma Membrane*

Cholesterol and diunsaturated forms of phospholipids have been shown to favor hexagonal $H_{II}$ phase formation in model membranes (Chen and Rand, 1997; Epand *et al*., 2003, 2005). The presence of $H_{II}$ promoting lipids results in curvature stress, a biophysical parameter of membranes that has been reported to regulate the folding and/or activity of integral proteins (for reviews, see Lee, 2003; van den Brink-van der Laan *et al*., 2004). Therefore, we wondered whether hexagonal $H_{II}$ phase formation could be an important parameter for normal Fur4p delivery to the plasma membrane. To test this hypothesis, Fur4p biogenesis was evaluated in a strain depleted of PE, a nonbilayer forming phospholipid with a high propensity to form a hexagonal $H_{II}$ phase. For this purpose, Fur4p was expressed in the *psd1*Δ *psd2*Δ *dpl1*Δ triple mutant strain RY200T. This strain is unable to synthesize PE except if the medium is supplemented with ethanolamine (Robl *et al*., 2001). In the PE depletion protocol used (Opekarova *et al*., 2005), RY200T cells were cultivated in YPRaff medium containing 2 mM ethanolamine and were transferred to YPGal + 2 mM ethanolamine (PE-competent cells) or YPGal + 4 mM choline (PE-depleted cells) for 16 h. Then, the cellular distribution of the Fur4p-GFP signal was observed by confocal microscopy. As shown in Figure 11A, whereas Fur4p-GFP was detected at the cell periphery in PE-competent cells, it accumulated in intracellular compart-

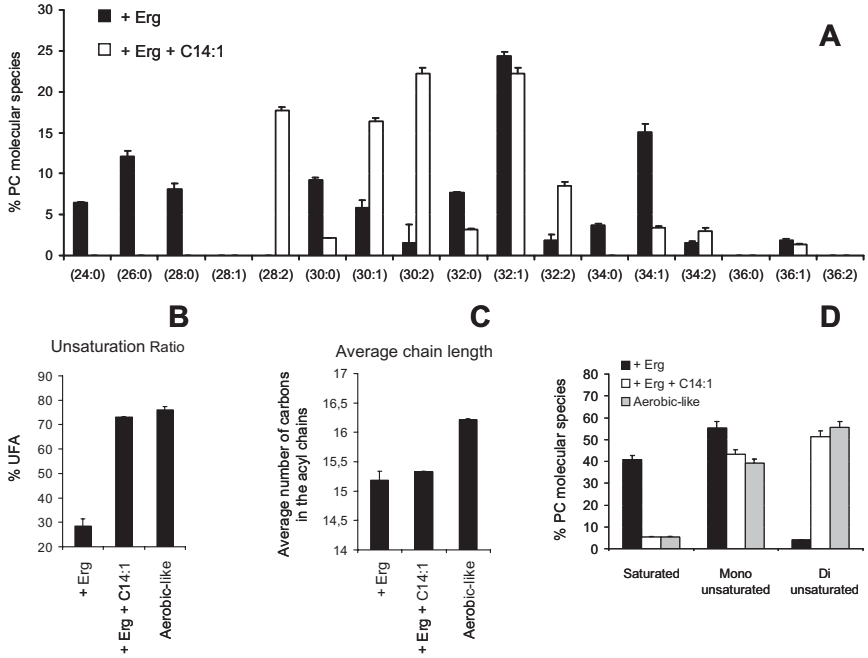


**Figure 10.** PC composition of *hem1*Δ grown in myristoleic acid-supplemented medium. *hem1*Δ cells were grown in the media indicated for 7 h before lipid extraction and MS analysis of PC species in the positive ion mode. (A) Relative abundance of molecular PC species. (B) Unsaturation ratio. (C) Average chain length. (D) Relative percentage of saturated versus monounsaturated and diunsaturated species. See legend of Figure 7 and text for details. Values are means ± S. D. of at least three independent measurements.

ments under PE depletion. To check whether Fur4p-GFP delivery to the plasma membrane was directly connected to the nonbilayer propensity of PE, the same experiment was performed in a medium in which ethanolamine was replaced by propanolamine (Prn). Indeed, Prn can be metabolized to phosphatidylpropanolamine in a *psd1*Δ *psd2*Δ strain, a phospholipid that cannot compensate fully for PE, because Prn cannot restore the growth of the RY200T *psd1*Δ *psd2*Δ *dpl1*Δ triple mutant strain, but that promotes hexagonal phase formation almost as efficiently as PE (Storey *et al*., 2001). As shown in Figure 11A, Fur4p-GFP was detected at the cell periphery in most of the RY200T cells grown on Prn, suggesting that hexagonal $H_{II}$ phase formation is indeed a critical parameter for Fur4p targeting to its final destination.

To provide some definition of the minimal PE levels required for plasma membrane sorting of Fur4p, the same experiment was performed with different concentrations of ethanolamine (0, 10 μM, 50 μM, 100 μM, 250 μM, 500 μM, 1 mM, or 2 mM ethanolamine). Interestingly, Fur4p-GFP could hardly be detected at the plasma membrane for ethanolamine concentrations below 250 μM (Figure 11B). In agreement with our previous observations (Figure 11A), addition of 2 mM propanolamine fully restored Fur4p-GFP sorting to the cell periphery under limiting ethanolamine concentrations (100 μM ethanolamine; Figure 11B). Direct determination of PE levels revealed a strict connection between the concentrations of exogenously supplied ethanolamine and cellular PE amounts (Figure 11C). The minimal PE concentration for efficient Fur4p-GFP delivery to the cell surface was estimated to 7.9 ± 1.0 nmol FA/$10^9$ cells, a concentration obtained under addition of 250 μM ethanolamine to the medium. This concentration corresponds to approximately one fourth of the PE levels detected in the RY2000T strain grown under optimal conditions (i.e., in the presence of 2 mM ethanolamine, 31.3 ± 1.8 nmol FA/$10^9$ cells; Figure 11C) and 1/14 of PE amounts in the reference

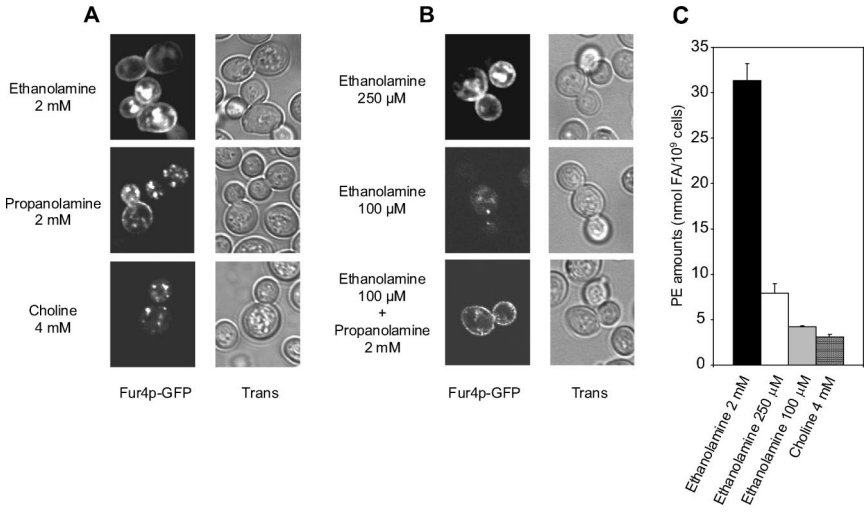


**Figure 11.** Phosphatidylethanolamine is required for optimal delivery of Fur4p-GFP to the plasma membrane. *RY200T* [pFl38gF-GFP] cells were grown for 16 h in YPGal medium supplemented (A) with ethanolamine (2 mM), choline (4 mM) or propanolamine (2 mM) and (B) with ethanolamine (250 μM), ethanolamine (50 μM) or ethanolamine (100 μM) + propanolamine (2 mM). Visualization of GFP fluorescence was performed by confocal microscopy. Trans, transmission. (C) *RY200T* cells were grown as in A, in the presence of the indicated supplements. PE concentrations as nanomoles of FA/$10^9$ cells were determined as described in *Materials and Methods*. Values are means ± S.D. of at least three independent determinations.

Y10000 wild-type strain, grown in YPGal medium without addition (110.4 ± 7.2 nmol FA/$10^9$ cells; data not shown).

## DISCUSSION

In the present study, we have evaluated the impact of ergosterol or UFA depletion on the biogenesis of the model polytopic membrane protein Fur4p. In the dynamic system used, Fur4p fails to be delivered to the plasma membrane when sterol amounts decrease below a critical concentration of ~4.5 ± 1.2 μg ergosterol/$10^9$ cells (Figures 1B and 6A). Under these conditions, Fur4p falls prey to a quality control system that displays all the characteristics of the Golgi-based quality control process: 1) Fur4p is sorted to the endosomal pathway without prior targeting to the plasma membrane (Figures 2D and 3A), 2) Fur4p is protected from degradation when accumulated in the Golgi apparatus (Figure 3B), and 3) is internalized in the vacuolar lumen in a Rsp5p-dependent manner (Figure 3C). This is a new example of the influence of sterols on the biogenesis of a membrane-associated protein.

Another important finding of this study is that the fatty acyl content of phospholipids influences Fur4p biogenesis. Indeed, as observed upon ergosterol scarcity, heme-induced UFA shortage resulted in Fur4p sorting to the endosomal pathway. To our knowledge, this is the first time that such an effect of cellular fatty acyl composition on the biogenesis of an integral protein is reported. ESI-MS analysis of phospholipid species revealed that UFA starvation induced two distinct responses on the fatty acyl content, i.e., a decrease in the unsaturation ratio and a shortening of the chain length (Figure 7). These effects are not related to an indirect consequence of heme depletion, but they are rather directly connected to the impaired fatty acid desaturation. Indeed, all three phenomena, i.e., Fur4p failure to reach the cell surface, a decrease in the unsaturation ratio, and the shortening of fatty acyl chains, were observed in an *ole1*Δ strain when grown without supplementation with an exogenous UFA source (unpublished data).

Shortening of the fatty acyl chains in phospholipids may represent an adaptation process to impaired desaturation. Yeast has already been reported to adjust its unsaturation level and the length of its phospholipid fatty acyl chains in response to various stresses such as temperature variations (Suutari *et al*., 1997) or conditions of PC depletion (Boumann *et al*., 2006). If one considers the potential effects of saturated fatty acid (SFA) accumulation in phospholipids under haem deficiency, one may expect a dramatic decrease in membrane fluidity, which is not compatible with most of the cellular processes that require high membrane dynamics. Shortening the acyl chains in phospholipids under these conditions may contribute to maintaining the membranes in the Ld state. This may explain why essential cellular processes such as secretion are still fully functional under lipid depletion, as judged by invertase secretion assays and Pma1p biogenesis studies (Figure 4).

A major question that arose from our observations was how depleting the cells of ergosterol or UFA, which were found to differently impact the overall lipid composition (Figures 6 and 7), could have the same effects on the biogenesis of a plasma membrane protein, such as Fur4p. The most reasonable hypothesis is that they influence a specific physical parameter of the lipid bilayer in the same way, e.g., domain formation, such as Lo/DRMs/raft domains, membrane fluidity, thickness, or intrinsic curvature.

Based on recent literature, we initially hypothesized that the disruption of raft domains could account for Fur4p recognition by the Golgi quality control process. However, this is obviously not the case, because the pattern of Fur4p association to DRMs was identical under aerobic-like and lipid-depleted conditions (Figure 3D). This was confirmed for individual ergosterol and UFA depletions (our unpublished data). Moreover, the association of another protein, Pma1p, to DRMs was also shown not to be impaired under the various lipid depletions (Figure 3D; our unpublished data). Pma1p association to DRMs has been proposed to be a prerequisite for plasma membrane delivery and stability (Bagnat *et al*., 2001; Pizzirusso and Chang, 2004; Gaigg *et al*., 2005, 2006). Accordingly, Pma1p targeting to the cell periphery was not abolished under ergosterol and UFA shortage (Figure 4).

If ergosterol scarcity and short saturated fatty acyl chain accumulation in phospholipids upon UFA depletion were not compatible with unidirectional changes in membrane fluidity, they may influence membrane width in the same way, by reducing bilayer thickness. Thickness of the hydrophobic membrane-spanning regions of an integral protein should match the thickness of the bilayer to avoid exposure of hydrophobic residues to water, a phenomenon known as hydrophobic-mismatch (for review, see Lee, 2003). However, such a phenomenon cannot account for our results with Fur4p. Indeed, we could show that the permease escapes the Golgi quality control process when grown in the presence of a short unsaturated fatty acid, myristoleic acid (Figure 9, + Erg + C14:1). Such an addition restored the phospholipid unsaturation ratio to a level equivalent to what was observed under aerobiosis-like conditions (Figure 10B), but it maintained a low average fatty acyl chain length (Figure 10C). Therefore, the unsaturation ratio of phospholipids seems to be a more critical parameter for Fur4p cell surface delivery than membrane width.

A model that fully accounts for our results is membrane curvature (van den Brink-van der Laan *et al*., 2004; de Kroon, 2007). Some phospholipids such as PC display an overall cylindrical shape and tend to organize themselves in bilayers. In contrast, other phospholipids such as PE display conical shapes (type II lipids), and they tend to form nonlamellar phases with a negative curvature such as the hexagonal phase $H_{II}$. When present in phospholipid bilayers, hexagonal phase-promoting lipids result in curvature stress, an overall property of the membrane that can influence the structure and activity of membrane-anchored proteins (for reviews, see Booth, 2003; van den Brink-van der Laan *et al*., 2004). It has been proposed that the presence of nonbilayer lipids may result in increased lateral pressure in the acyl chain region that could favor the packing of transmembrane helices (van den Brink-van der Laan *et al*., 2004). Interestingly, increasing the amount of diunsaturated PC species and the relative cholesterol concentration augments the propensity of PC/cholesterol mixtures to form an $H_{II}$ phase in model membranes (Epand *et al*., 2003, 2005; Tenchov *et al*., 2006). Moreover, the accumulation of short saturated fatty acid chains in PE in yeast has been shown to remarkably decrease its $H_{II}$ phase propensity due to a reduction of its overall conical shape (Boumann *et al*., 2006). Therefore, based on these observations, one may expect that ergosterol and UFA shortage, through a decrease in diunsaturated PC (Figure 7D) and PE (unpublished data) species in favor of saturated forms, induce unidirectional changes in membrane curvature, i.e., a decrease in curvature stress. The hypothesis for such a direct connection between curvature stress and optimal Fur4p delivery to the plasma membrane is strengthened by the observed deleterious effects of PE depletion on Fur4p biogenesis (Figure 11), effects that can be rescued in part by replacing PE with the $H_{II}$ hexagonal

phase promoter phosphatidylpropanolamine (Figure 11; Storey *et al*., 2001).

Finally, the results presented in this study point to the Golgi apparatus being a major compartment for lipid-mediated controlled cell surface delivery of plasma membrane proteins. In this respect, the fact that Pma1p trafficking to the cell periphery is not abolished under lipid depletion (Figure 4) suggests that Fur4p and Pma1p are not equally sensitive to changes in the lipid environment. This may be related to unique immediate lipid surroundings that may account for their different sensitivities to Triton X-100 solubilization (Figure 3D), or a different oligomerization status of these two proteins. Lipid-mediated early segregation at the Golgi level could account, at least in part, for Fur4p and Pma1p localizations to distinct plasma membrane subdomains (Malinska *et al*., 2004; Grossmann *et al*., 2007). In this context, modifying curvature stress may be a way to regulate the delivery of selective plasma membrane proteins to their final destination.

## ACKNOWLEDGMENTS

We thank Jenny Colas for excellent technical assistance, Dr. Anne Cantereau for precious advice regarding confocal microscopy imaging, Dr. Patrick Mazellier for help and comments with phospholipid analysis by tandem mass spectrometry. We thank Drs. Randy Schekman, Carolyn Slayman, Miroslava Opekarova (Institute of Microbiology, Prague, Czech Republic), Teresa Zoladek (Institute of Biochemistry and Biophysics, Warsaw, Poland), and Rosine Haguenauer-Tsapis (Institut Jacques Monod, Paris, France) for strains, plasmids, and antibodies. Drs. Danièle Urban-Grimal and Elsa Lauwers are also acknowledged for protocols concerning DRM preparation and for sharing preliminary results. Dr. Manilduth Ramnath provided helpful comments concerning the manuscript and Dr. Elizabeth Pilon-Smits improved the language. This work was supported by the French MENRT (with a grant to L.P), the Conseil Général de la Région Poitou-Charente and the CNRS.

## REFERENCES

Bagnat, M., Chang, A., and Simons, K. (2001). Plasma membrane proton ATPase pma1p requires raft association for surface delivery in yeast. Mol. Biol. Cell *12*, 4129–4138.

Bagnat, M., Keranen, S., Shevchenko, A., and Simons, K. (2000). Lipid rafts function in biosynthetic delivery of proteins to the cell surface in yeast. Proc. Natl. Acad. Sci. USA *97*, 3254–3259.

Benedetti, H., Raths, S., Crausaz, F., and Riezman, H. (1994). The END3 gene encodes a protein that is required for the internalization step of endocytosis and for actin cytoskeleton organization in yeast. Mol. Biol. Cell *5*, 1023–1037.

Blondel, M.-O., Morvan, J., Dupre, S., Urban-Grimal, D., Haguenauer-Tsapis, R., and Volland, C. (2004). Direct sorting of the yeast uracil permease to the endosomal system is controlled by uracil binding and Rsp5p-dependent ubiquitylation. Mol. Biol. Cell *15*, 883–895.

Booth, P. J. (2003). The trials and tribulations of membrane protein folding in vitro. Biochim. Biophys. Acta *1610*, 51–56.

Boumann, H. A., Gubbens, J., Koorengevel, M. C., Oh, C.-S., Martin, C. E., Heck, A.J.R., Patton-Vogt, J., Henry, S. A., de Kruijff, B., and de Kroon, A.I.P.M. (2006). Depletion of phosphatidylcholine in yeast induces shortening and increased saturation of the lipid acyl chains: evidence for regulation of intrinsic membrane curvature in a eukaryote. Mol. Biol. Cell *17*, 1006–1017.

Brown, D. A., and London, E. (2000). Structure and function of sphingolipid- and cholesterol-rich membrane rafts. J. Biol. Chem. *275*, 17221–17224.

Buede, R., Rinker-Schaffer, C., Pinto, W. J., Lester, R. L., and Dickson, R. C. (1991). Cloning and characterization of LCB1, a Saccharomyces gene required for biosynthesis of the long-chain base component of sphingolipids. J. Bacteriol. *173*, 4325–4332.

Chen, Z., and Rand, R. P. (1997). The influence of cholesterol on phospholipid membrane curvature and bending elasticity. Biophys. J. *73*, 267–276.

Daum, G., Lees, N. D., Bard, M., and Dickson, R. (1998). Biochemistry, cell biology and molecular biology of lipids of *Saccharomyces cerevisiae*. Yeast *14*, 1471–1510.

de Kroon, A.I.P.M. (2007). Metabolism of phosphatidylcholine and its implications for lipid acyl chain composition in *Saccharomyces cerevisiae*. Biochim. Biophys. Acta *1771*, 343–352.

DeWitt, N. D., dos Santos, C.F.T., Allen, K. E., and Slayman, C. W. (1998). Phosphorylation region of the yeast plasma-membrane H+-ATPase. role in protein folding and biogenesis. J. Biol. Chem. *273*, 21744–21751.

Dickson, R. C., Sumanasekera, C., and Lester, R. L. (2006). Functions and metabolism of sphingolipids in *Saccharomyces cerevisiae*. Prog. Lipid Res. *45*, 447–465.

Dupre, S., and Haguenauer-Tsapis, R. (2003). Raft partitioning of the yeast uracil permease during trafficking along the endocytic pathway. Traffic *4*, 83–96.

Dupre, S., Urban-Grimal, D., and Haguenauer-Tsapis, R. (2004). Ubiquitin and endocytic internalization in yeast and animal cells. Biochim. Biophys. Acta *1695*, 89–111.

Epand, R. M., Epand, R. F., Hughes, D. W., Sayer, B. G., Borochov, N., Bach, D., and Wachtel, E. (2005). Phosphatidylcholine structure determines cholesterol solubility and lipid polymorphism. Chem. Physics Lipids *135*, 39–53.

Epand, R. M., Hughes, D. W., Sayer, B. G., Borochov, N., Bach, D., and Wachtel, E. (2003). Novel properties of cholesterol-dioleoylphosphatidylcholine mixtures. Biochim. Biophys. Acta *1616*, 196–208.

Ferreira, T., Mason, A. B., Pypaert, M., Allen, K. E., and Slayman, C. W. (2002). Quality control in the yeast secretory pathway. A misfolded PMA1 H+-ATPase reveals two checkpoints. J. Biol. Chem. *277*, 21027–21040.

Ferreira, T., Regnacq, M., Alimardani, P., Moreau-Vauzelle, C., and Berges, T. (2004). Lipid dynamics in yeast under haem-induced unsaturated fatty acid and / or sterol depletion. Biochem. J. *378*, 899–908.

Folch, J., Lees, M., and Stanley, G.H.S. (1957). A simple method for the isolation and purification of total lipides from animal tissues. J. Biol. Chem. *226*, 497–509.

Gabriely, G., Kama, R., and Gerst, J. E. (2007). Involvement of specific COPI subunits in protein sorting from the late endosome to the vacuole in yeast. Mol. Cell. Biol. *27*, 526–540.

Gaigg, B., Timischl, B., Corbino, L., and Schneiter, R. (2005). Synthesis of sphingolipids with very long chain fatty acids but not ergosterol is required for routing of newly synthesized plasma membrane ATPase to the cell surface of yeast. J. Biol. Chem. *280*, 22515–22522.

Gaigg, B., Toulmay, A., and Schneiter, R. (2006). Very long-chain fatty acid-containing lipids rather than sphingolipids per se are required for raft association and stable surface transport of newly synthesized plasma membrane ATPase in yeast. J. Biol. Chem. *281*, 34135–34145.

Grossmann, G., Opekarova, M., Malinsky, J., Weig-Meckl, I., and Tanner, W. (2007). Membrane potential governs lateral segregation of plasma membrane proteins and lipids in yeast. EMBO J. *26*, 1–8.

Hearn, J. D., Lester, R. L., and Dickson, R. C. (2003). The uracil transporter Fur4p associates with lipid rafts. J. Biol. Chem. *278*, 3679–3686.

Hein, C., Springael, J. Y., Volland, C., Haguenauer-Tsapis, R., and Andre, B. (1995). NPl1, an essential yeast gene involved in induced degradation of Gap1 and Fur4 permeases, encodes the Rsp5 ubiquitin-protein ligase. Mol. Microbiol. *18*, 77–87.

Helms, J. B., and Zurzolo, C. (2004). Lipids as targeting signals: lipid rafts and intracellular trafficking. Traffic *5*, 247–254.

Henneberry, A. L., Lagace, T. A., Ridgway, N. D., and McMaster, C. R. (2001). Phosphatidylcholine synthesis influences the diacylglycerol homeostasis required for SEC14p-dependent Golgi function and cell growth. Mol. Biol. Cell *12*, 511–520.

Hoekstra, D., and van IJzendoorn, S. C. (2000). Lipid trafficking and sorting: how cholesterol is filling gaps. Curr. Opin. Cell Biol. *12*, 496–502.

Jacobson, K., Mouritsen, O. G., and Anderson, R.G.W. (2007). Lipid rafts: at a crossroad between cell biology and physics. Nat. Cell. Biol. *9*, 7–14.

Kaliszewski, P., Ferreira, T., Gajewska, B., Szkopinska, A., Berges, T., and Zoladek, T. (2006). Enhanced levels of Pis1p (phosphatidylinositol synthase) improve the growth of *Saccharomyces cerevisiae* cells deficient in Rsp5 ubiquitin ligase. Biochem. J. *395*, 173–181.

Katzmann, D. J., Odorizzi, G., and Emr, S. D. (2002). Receptor downregulation and multivesicular-body sorting. Nat. Rev. Mol. Cell Biol. *3*, 893–905.

Katzmann, D. J., Sarkar, S., Chu, T., Audhya, A., and Emr, S. D. (2004). Multivesicular body sorting: ubiquitin ligase Rsp5 is required for the modification and sorting of carboxypeptidase S. Mol. Biol. Cell *15*, 468–480.

Lauwers, E., and Andre, B. (2006). Association of yeast transporters with detergent-resistant membranes correlates with their cell-surface location. Traffic *7*, 1045–1059.

Lee, A. G. (2003). Lipid-protein interactions in biological membranes: a structural perspective. Biochim. Biophys. Acta *1612*, 1–40.

Lee, M. C., Hamamoto, S., and Schekman, R. (2002). Ceramide biosynthesis is required for the formation of oligomeric H+-ATPase, Pma1p, in the yeast endoplasmic reticulum. J. Biol. Chem. *11*, 22395–22401.

London, E. (2005). How principles of domain formation in model membranes may explain ambiguities concerning lipid raft formation in cells. Biochim. Biophys. Acta *1746*, 203–220.

Malinska, K., Malinsky, J., Opekarova, M., and Tanner, W. (2003). Visualization of protein compartmentation within the plasma membrane of living yeast cells. Mol. Biol. Cell *14*, 4427–4436.

Malinska, K., Malinsky, J., Opekarova, M., and Tanner, W. (2004). Distribution of Can1p into stable domains reflects lateral protein segregation within the plasma membrane of living *S. cerevisiae* cells. J. Cell Sci. *117*, 6031–6041.

Marchal, C., Dupre, S., and Urban-Grimal, D. (2002). Casein kinase I controls a late step in the endocytic trafficking of yeast uracil permease. J. Cell Sci. *115*, 217–226.

Morvan, J., Froissard, M., Haguenauer-Tsapis, R., and Urban-Grimal, D. (2004). The ubiquitin ligase Rsp5p is required for modification and sorting of membrane proteins into multivesicular bodies. Traffic *5*, 383–392.

Munn, A. L., Heese-Peck, A., Stevenson, B. J., Pichler, H., and Riezman, H. (1999). Specific sterols required for the internalization step of endocytosis in yeast. Mol. Biol. Cell *10*, 3943–3957.

Munro, S. (2003). Lipid rafts: elusive or illusive? Cell *115*, 377–388.

Opekarova, M., Malinska, K., Novakova, L., and Tanner, W. (2005). Differential effect of phosphatidylethanolamine depletion on raft proteins: further evidence for diversity of rafts in *Saccharomyces cerevisiae*. Biochim. Biophys. Acta *1711*, 87–95.

Opekarova, M., Robl, I., and Tanner, W. (2002). Phosphatidyl ethanolamine is essential for targeting the arginine transporter Can1p to the plasma membrane of yeast. Biochim. Biophys. Acta *1564*, 9–13.

Pizzirusso, M., and Chang, A. (2004). Ubiquitin-mediated targeting of a mutant plasma membrane ATPase, Pma1–7, to the endosomal/vacuolar system in yeast. Mol. Biol. Cell *15*, 2401–2409.

Robl, I., Grassl, R., Tanner, W., and Opekarova, M. (2001). Construction of phosphatidylethanolamine-less strain of *Saccharomyces cerevisiae*. Effect on amino acid transport. Yeast *18*, 251–260.

Schneiter, R. *et al*. (1999). Electrospray ionization tandem mass spectrometry (ESI-MS/MS) analysis of the lipid molecular species composition of yeast subcellular membranes reveals acyl chain-based sorting/remodeling of distinct molecular species en route to the plasma membrane. J. Cell Biol. *146*, 741–754.

Storey, M. K., Clay, K. L., Kutateladze, T., Murphy, R. C., Overduin, M., and Voelker, D. R. (2001). Phosphatidylethanolamine has an essential role in *Saccharomyces cerevisiae* that is independent of its ability to form hexagonal phase structures. J. Biol. Chem. *276*, 48539–48548.

Suutari, M., Rintamaki, A., and Laakso, S. (1997). Membrane phospholipids in temperature adaptation of *Candida utilis*: alterations in fatty acid chain length and unsaturation. J. Lipid Res. *38*, 790–794.

Tenchov, B. G., MacDonald, R. C., and Siegel, D. P. (2006). Cubic phases in phosphatidylcholine-cholesterol mixtures: cholesterol as membrane "Fusogen." Biophys. J. *91*, 2508–2516.

Umebayashi, K., and Nakano, A. (2003). Ergosterol is required for targeting of tryptophan permease to the yeast plasma membrane. J. Cell Biol. *161*, 1117–1131.

Valdez-Taubas, J., and Pelham, H. R. (2003). Slow diffusion of proteins in the yeast plasma membrane allows polarity to be maintained by endocytic cycling. Curr. Biol. *13*, 1636–1640.

van den Brink-van der Laan, E., Antoinette Killian, J., and de Kruijff, B. (2004). Nonbilayer lipids affect peripheral and integral membrane proteins via changes in the lateral pressure profile. Biochim. Biophys. Acta *1666*, 275–288.

Verdiere, J., Gaisne, M., and Labbe-Bois, R. (1991). CYP1 (HAP1) is a determinant effector of alternative expression of heme-dependent transcribed genes in yeast. Mol. Gen. Genet. *228*, 300–306.

Vida, T. A., and Emr, S. D. (1995). A new vital stain for visualizing vacuolar membrane dynamics and endocytosis in yeast. J. Cell Biol. *128*, 779–792.

Volland, C., Urban-Grimal, D., Geraud, G., and Haguenauer-Tsapis, R. (1994). Endocytosis and degradation of the yeast uracil permease under adverse conditions. J. Biol. Chem. *269*, 9833–9841.

Wang, Q., and Chang, A. (2002). Sphingoid base synthesis is required for oligomerization and cell surface stability of the yeast plasma membrane ATPase, Pma1. Proc. Natl. Acad. Sci. USA *20*, 12853–12858.

Woolford, C. A., Daniels, L. B., Park, F. J., Jones, E. W., Van Arsdell, J. N., and Innis, M. A. (1986). The PEP4 gene encodes an aspartyl protease implicated in the posttranslational regulation of *Saccharomyces cerevisiae* vacuolar hydrolases. Mol. Cell. Biol. *6*, 2500–2510.